

# Synthesis and Evaluation of a Novel Library of Alternating Amphipathic Copolymers to Solubilize and Study Membrane Proteins

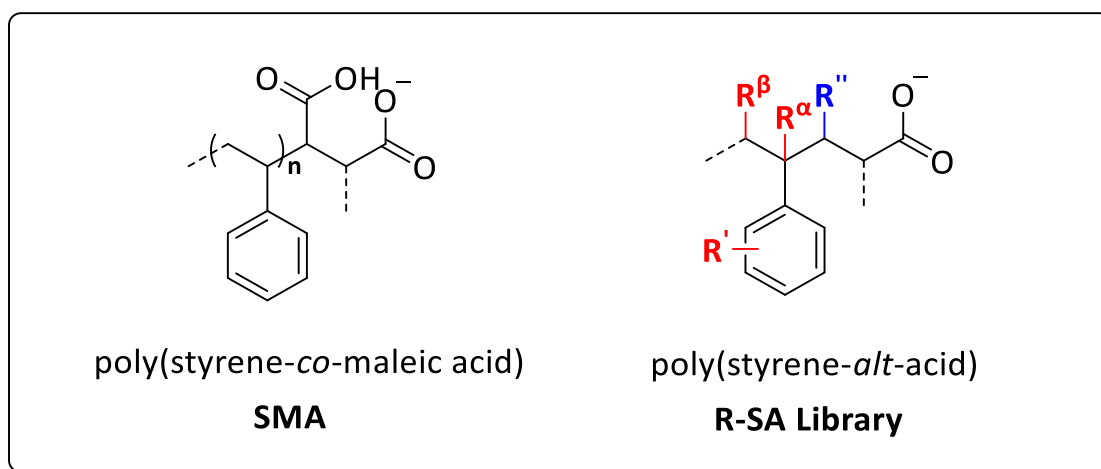
Adrian H. Kopf,\* Odette Lijding, Barend O. W. Elenbaas, Martijn C. Koorengevel, Cornelis A. van Walree, J. Antoinette Killian,\*

Membrane Biochemistry and Biophysics, Bijvoet Center for Biomolecular Research, Institute of Biomembranes, Utrecht University, Padualaan 8, 3584 CH Utrecht, The Netherlands.

\* Corresponding authors. *E-mail addresses:* [a.h.kopf@uu.nl](mailto:a.h.kopf@uu.nl) (A.H.Kopf), [j.a.killian@uu.nl](mailto:j.a.killian@uu.nl) (J.A.Killian).

## Abstract

Amphipathic copolymers such as poly(styrene-maleic acid) (SMA) are promising tools for the facile extraction of membrane proteins (MPs) into native nanodiscs. Here, we designed and synthesized a library of well-defined alternating copolymers of SMA analogues in order to elucidate polymer properties that are important for MP solubilization and stability. MP extraction efficiency was determined using KcsA from *E.coli* membranes and general solubilization efficiency was investigated via turbidimetry experiments on membranes of *E.coli*, yeast mitochondria and synthetic lipids. Remarkably, halogenation of SMA copolymers dramatically improved solubilization efficiency in all systems, while substituents on the copolymer backbone improved resistance to  $\text{Ca}^{2+}$ . Relevant polymer properties were found to include hydrophobic balance, size and positioning of substituents, rigidity and electronic effects. The library thus contributes to the rational design of copolymers for the study of MPs.



Graphical Abstract

## Keywords

Amphipathic copolymers, copolymer design, membrane proteins, native nanodiscs, polymers

## Abbreviations

MPs, Membrane Proteins; SMAnh, Styrene-Maleic Anhydride; SMA, Styrene-Maleic Acid; SA, Styrene-Acid; Đ, Dispersity; RAFT, Reversible-Addition-Fragmentation Transfer.

## Introduction

Membrane proteins (MPs) have a prominent biological and pharmacological importance. Nevertheless, their structures remain highly underrepresented as compared to those of water-soluble proteins,<sup>[1][2]</sup> mainly because MPs tend to destabilize when taken out of their native lipid environment. The use of styrene-maleic acid (SMA) copolymers, as first described in 2009,<sup>[3]</sup> has given a substantial impetus to the field of MP research, as these amphipathic polymers can solubilize MPs together with an annulus of native lipids, forming so-called native nanodiscs.<sup>[4][5][6][7]</sup> This preservation of the endogenous lipidic environment confers high stability to the MPs, and allows for the study of (native) lipid-protein and protein-protein interactions.<sup>[7][8][9][10][11]</sup> The MPs in the nanodiscs furthermore are amenable to functional and structural studies with an array of biophysical techniques,<sup>[12]</sup> including mass spectrometry,<sup>[13]</sup> mass photometry,<sup>[14]</sup> NMR spectroscopy,<sup>[15][16]</sup> and cryo-electron microscopy.<sup>[5][17][18]</sup>

The efficiency of membrane solubilization by SMA copolymers is determined by many factors, including environmental conditions such as ionic strength and pH,<sup>[19][20]</sup> physicochemical properties of the target membrane<sup>[21][22][23]</sup> and properties of SMA, such as length and chemical composition.<sup>[24][25][26][20]</sup> Copolymers with relatively short chains<sup>[24][27]</sup> and with a ratio of styrene-to-maleic acid of ~2:1 and ~3:1<sup>[20][28]</sup> generally are efficient at solubilization, while either more hydrophobic (~4:1) or more hydrophilic (~1:1) copolymers are not.<sup>[25][26][20]</sup>

Unfortunately, SMA copolymers that are efficient solubilizers (i.e. with a ~2:1 or 3:1 styrene-to-maleic acid ratio) tend to be very heterogeneous in size<sup>[27][29]</sup> and composition,<sup>[24][20]</sup> with a highly irregular distribution of comonomers along the copolymer backbone.<sup>[24]</sup> This is because during copolymerization styrene and maleic-anhydride prefer to form alternating (1:1) copolymers and because the polymers are synthesized in a free-radical copolymerization reaction, which is a random process.<sup>[29][30][31]</sup> To facilitate studies on MP solubilization by SMA, much work has been performed on preparing copolymers with more uniform size dispersity and/or with well-defined comonomer sequence distributions.<sup>[24][27][32][33][34][35]</sup> Furthermore, by introducing various substitutions,<sup>[36][37][38]</sup> different types of copolymers have been developed to overcome some of the limitations of SMA, e.g. enabling use in a different pH range or in the presence of divalent cations.<sup>[39][40][41][42][43]</sup> However, these copolymers are not always effective solubilizers and ultimately a clearer understanding that allows for a more comprehensive predictive and rational design has remained elusive.

Here, we present a library of well-defined, alternating (1:1) amphipathic copolymers with systematic substitutions to allow elucidation of polymer parameters that are important for biologically relevant properties, such as solubilization efficiency and divalent cation resistance. The new library expands the toolkit available for the isolation and characterization of MPs.

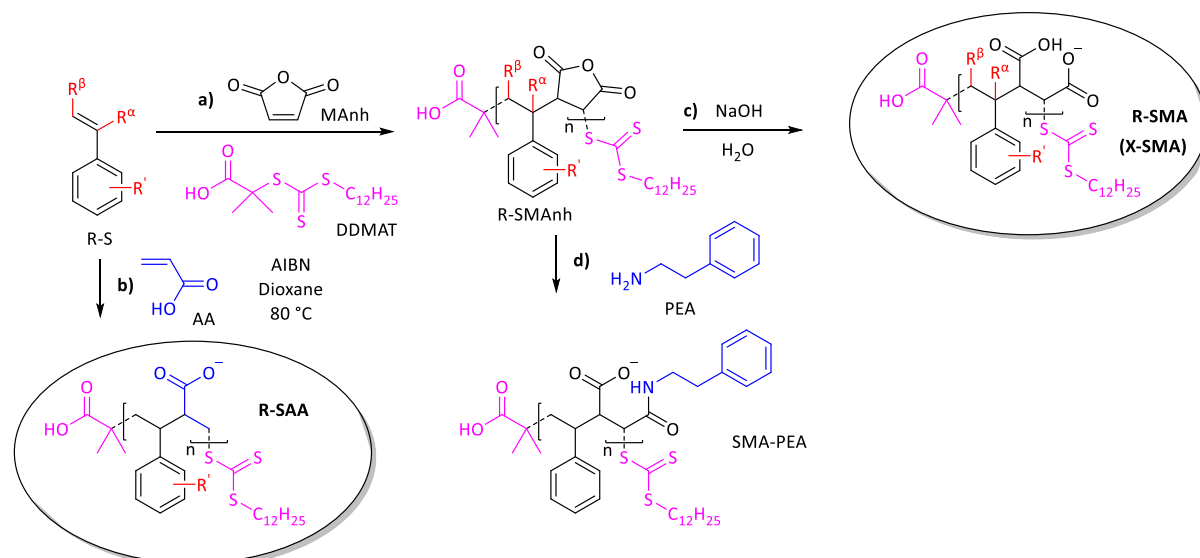
## Results and Discussion

### Synthesis and characterization of a library of amphipathic copolymers

A library of amphipathic copolymers was synthesized according to the general procedure in Scheme 1. The aim was to make alternating SMA copolymer analogues that are more lipophilic, by systematic variation of their chemical composition. This was done by either using styrene analogues with a more hydrophobic non-polar moiety or by making the polar maleic acid moiety less hydrophilic.

Three sets of copolymers were synthesized in a living free-radical reaction via Reversible-Addition-Fragmentation Transfer (RAFT)-mediated copolymerization. **R-SMA** was synthesized by copolymerizing styrenic analogues (R-S) with maleic-anhydride (MAnh) to obtain R-SMAnh copolymers, followed by hydrolysis (Scheme 1a and 1c). It has modifications of the hydrophobic

moiety (highlighted in red), either on the pendant group ( $R'$ ) or the backbone ( $R^{\alpha/\beta}$ ). **X-SMA** is a special sub-set of R-SMA where the derivatives (R) represent halogen atoms (X). **R-SAA** has only one carboxylic acid group (highlighted in blue) and was obtained by copolymerization with acrylic acid (AA) (Scheme 1b). A separate type of modification is SMA-PEA, in which the copolymer was made less hydrophilic by opening the maleic anhydride rings with phenethylamine (PEA, highlighted in blue) (Scheme 1d).



Scheme 1: General synthetic scheme showing the synthesis of different sets of SMA analogues. Styrenic derivatives (R-S) were copolymerized either with maleic-anhydride (MAh) to obtain R-SMAh copolymers (a) or with acrylic acid (AA) to obtain R-SAA copolymers (b). Following copolymerization, R-SMAh parent copolymers were hydrolysed to the water-soluble free acid forms (R/X-SMA) under aqueous alkaline conditions (c). SMA-PEA was prepared by reacting SMAh with phenethylamine (PEA) (d). Comonomers were added at an equimolar concentration (1:1 mole ratio). Other reaction conditions included the use of azobisisobutyronitrile (AIBN) as radical source, 2-(dodecylthiocarbonothioylthio)-2-methylpropionic acid (DDMAT) as the RAFT agent (highlighted in pink), anhydrous dioxane as solvent, and a reaction temperature of 80 °C.

The modifications in the synthesized library are illustrated in Fig. 1 and the full chemical structures are shown in Fig. S1. Copolymerization and subsequent hydrolysis were confirmed by FT-IR and UV-vis spectroscopy (Fig. S2 and Fig. S3). Subsequently, copolymer size ( $M_n$ ,  $M_w$ ) and dispersity ( $\mathcal{D}$ ) were determined by Gel Permeation Chromatography (GPC) (Fig. S4). Table 1 summarizes the properties of the polymers. Most copolymers gave roughly the targeted peak sizes as well as good size distributions ( $\mathcal{D} < 1.3$ , as expected for RAFT polymerization, with only  $\alpha$ -MeSMA having a slightly larger  $\mathcal{D}$  of 1.57). For stilbene (StbMA) and beta-naphthalene ( $\beta$ -NMA), the GPC experiments showed bimodal distributions with the main peak coinciding with the anticipated smaller RAFT-copolymer size and  $\mathcal{D}$ . The second peak represented a much longer polymer and more disperse fraction, which could be due to standard free-radical polymerization occurring alongside living (RAFT) polymerization.

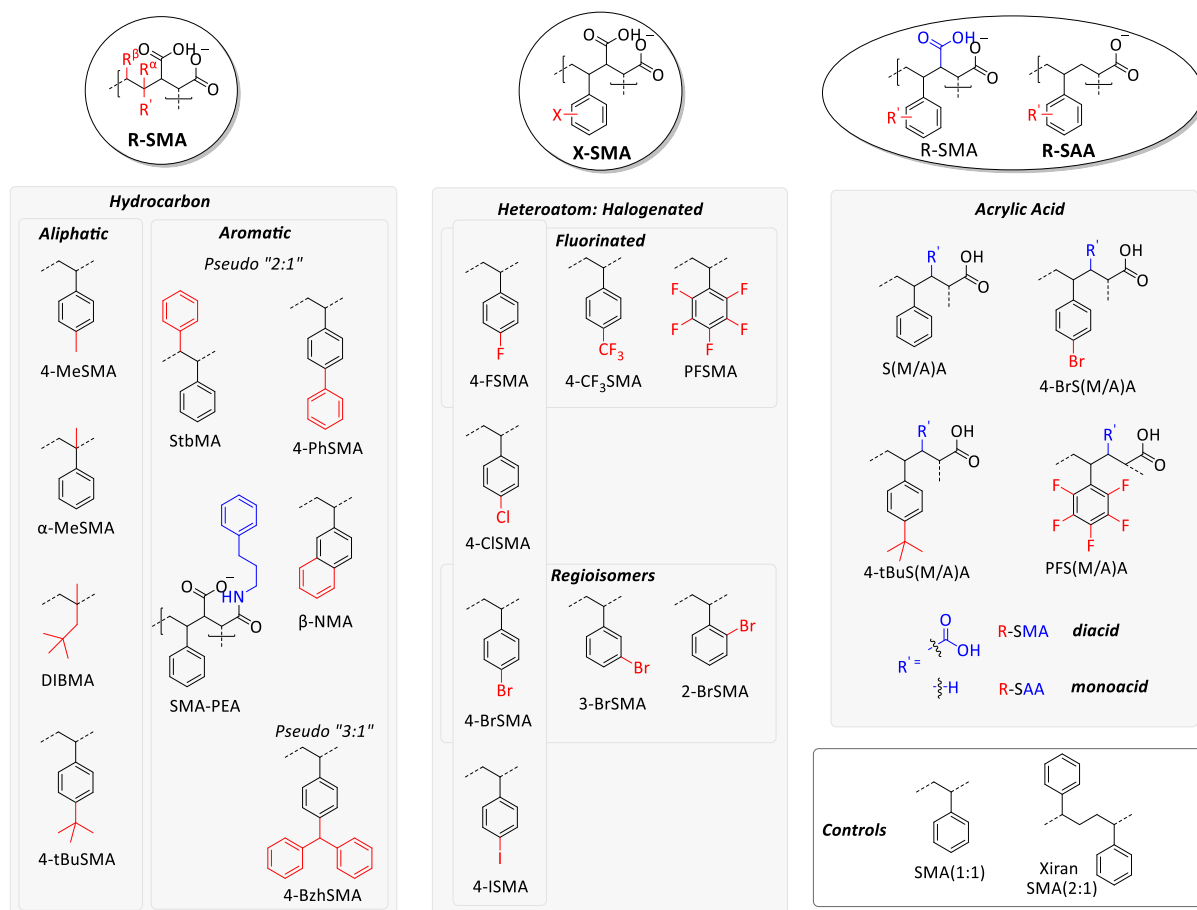


Fig. 1: Library of SMA copolymer analogues, showing the three different classes (R-SMA, X-SMA, and R-SAA) and their subdivisions. Modification of the styrene units are highlighted in red and of the hydrophilic units in blue.

Table 1: Characterization of RAFT synthesized amphipathic copolymers

#	Name	R	R <sup>α</sup>	R <sup>β</sup>	Hydrophilic Moiety	Yield (%)	D.P.	M <sub>n</sub> (kDa)	M <sub>w</sub> (kDa)	Đ
<b>R-SMA</b>										
1	SMA	H	H	H	MA	93	42	4.6	5.3	1.15
2	α-MeSMA	H	Me	H	MA	63	25	3.1	4.8	1.57
3	4-MeSMA	4-Me	H	H	MA	100	46	5.4	6.3	1.17
4	4-PhSMA	4-Ph	H	H	MA	71	24	3.8	4.9	1.29
5	4-BzhSMA	4-Bzh	H	H	MA	90	35	6.8	8.8	1.29
6	4-tBuSMA	4-tBu	H	H	MA	100	51	6.9	8.3	1.20
8	DIBMA	DIB	Me	H	MA	57	27	3.2	3.6	1.12
9	StbMA	H	H	Ph	MA	58	29, 1621 <sup>a</sup>	4.5, 226 <sup>a</sup>	5.3, 457 <sup>a</sup>	1.19, 2.02 <sup>a</sup>
10	β-NMA	Np	H	H	MA	70	16, 3315 <sup>b</sup>	2.4, 419 <sup>b</sup>	2.9, 1520 <sup>b</sup>	1.23, 3.63 <sup>b</sup>
11	SMA-PEA	H	H	H	AA-PEA	86	42	4.7	5.4	1.15
<b>X-SMA</b>										
12	SMA	H	H	H	MA	76	17	2.1	2.6	1.21
13	4-FSMA	4-F	H	H	MA	75	20	2.6	3.1	1.17
14	4-CISMA	4-Cl	H	H	MA	68	15	2.2	2.6	1.19
15	4-BrSMA	4-Br	H	H	MA	63	11	1.9	2.4	1.24
16	4-ISMA	4-I	H	H	MA	49	14	2.6*	-	-
17	3-BrSMA	3-Br	H	H	MA	61	11	1.9	2.3	1.21
18	2-BrSMA	2-Br	H	H	MA	64	13	2.2	2.6	1.16
19	4-CF <sub>3</sub> SMA	4-CF <sub>3</sub>	H	H	MA	77	14	2.3	2.7	1.17
20	PFSMA	2,3,4,5,6-F	H	H	MA	60	10	1.8	2.1	1.14
<b>R-SAA</b>										
21	SAA	H	H	H	AA	46	11	1.4	1.6	1.17
22	4-BrSAA	4-Br	H	H	AA	46	11	1.7	2.0	1.18
23	PFSAA	2,3,4,5,6-F	H	H	AA	60	18	2.7	3.2	1.18
24	4-tBuSAA	4-tBu	H	H	AA	59	23	3.0	3.8	1.25

D.P., Degree of Polymerization. M<sub>n</sub>, number average molecular weight. M<sub>w</sub>, weight average molecular weight. Đ, Dispersity. MA, Maleic Acid. AA, Acrylic Acid. <sup>a</sup>12% (AUC), <sup>b</sup>45% (AUC). \*Based on UV-vis measurements

### Efficiency of membrane protein solubilization from *E. coli*

The ability of the copolymers to solubilize biomembranes was first tested using the tetrameric K<sup>+</sup>-channel KcsA as a model protein, overexpressed in *Escherichia coli*.<sup>[7][19]</sup> The solubilization efficiency was quantified by densitometry on SDS-PAGE gels.<sup>[7][19]</sup> To create an optimal window for the evaluation of the efficacy of all substitutions, a relatively low concentration of copolymer (0.25% w/v) was used, at which the commercially available “gold standard” Xiran SZ30010, (SMA 2:1, styrene-to-maleic acid ratio) does not give complete solubilization.

#### R-SMA analogues

The first set of analogues, referred to as R-SMA, contains aliphatic or aromatic substituents to increase the hydrophobicity of the alternating SMA copolymers (Fig. 2A). As expected, SMA 2:1 yielded only partial solubilization (~42% KcsA extraction), while the unsubstituted SMA (alternating, 1:1) was unable to solubilize the membranes (<3%). The aliphatic copolymer DIBMA also showed negligible solubilization (~1%) under these sub-optimal conditions.

Homologues of (1:1) SMA containing an extra methyl group, either on the backbone in the α-position (α-MeSMA) or on the *para* position of the aromatic ring (4-MeSMA) gave slightly increased yields (~6%) compared to the underivatized SMA. Interestingly, a *tert*-butyl group on styrene (4-tBuSMA) showed a solubilization efficacy of ~55%, outperforming the commercial 2:1 SMA.

The aromatic substitutions yielded pseudo “2:1” SMA copolymers. Introduction of a second phenyl ring either by opening up the maleic anhydride ring using phenethylamine (SMA-PEA) or by grafting it

on the  $\beta$ -position of the backbone (StbMA), resulted in negligible solubilization ( $\sim 1\%$ ), in agreement with previous studies, where a StbMA copolymer was found to be ineffective in dissolving lipid vesicles.<sup>[44]</sup> However, when the phenyl was grafted directly to the styrene on the *para* position (4-PhSMA), the polymer had a solubilization efficacy of  $\sim 34\%$ . Finally an analogue where two aromatic rings are fused into a rigid naphthalene group ( $\beta$ -NMA) was found to be the best solubilizer ( $\sim 63\%$ ) in the series. The addition of another aromatic ring in the 3:1 mimic benzhydryl (4-BzhSMA) did not result in any membrane activity ( $\sim 0\%$ ), most likely because the groups are either too hydrophobic or too bulky for efficient insertion.

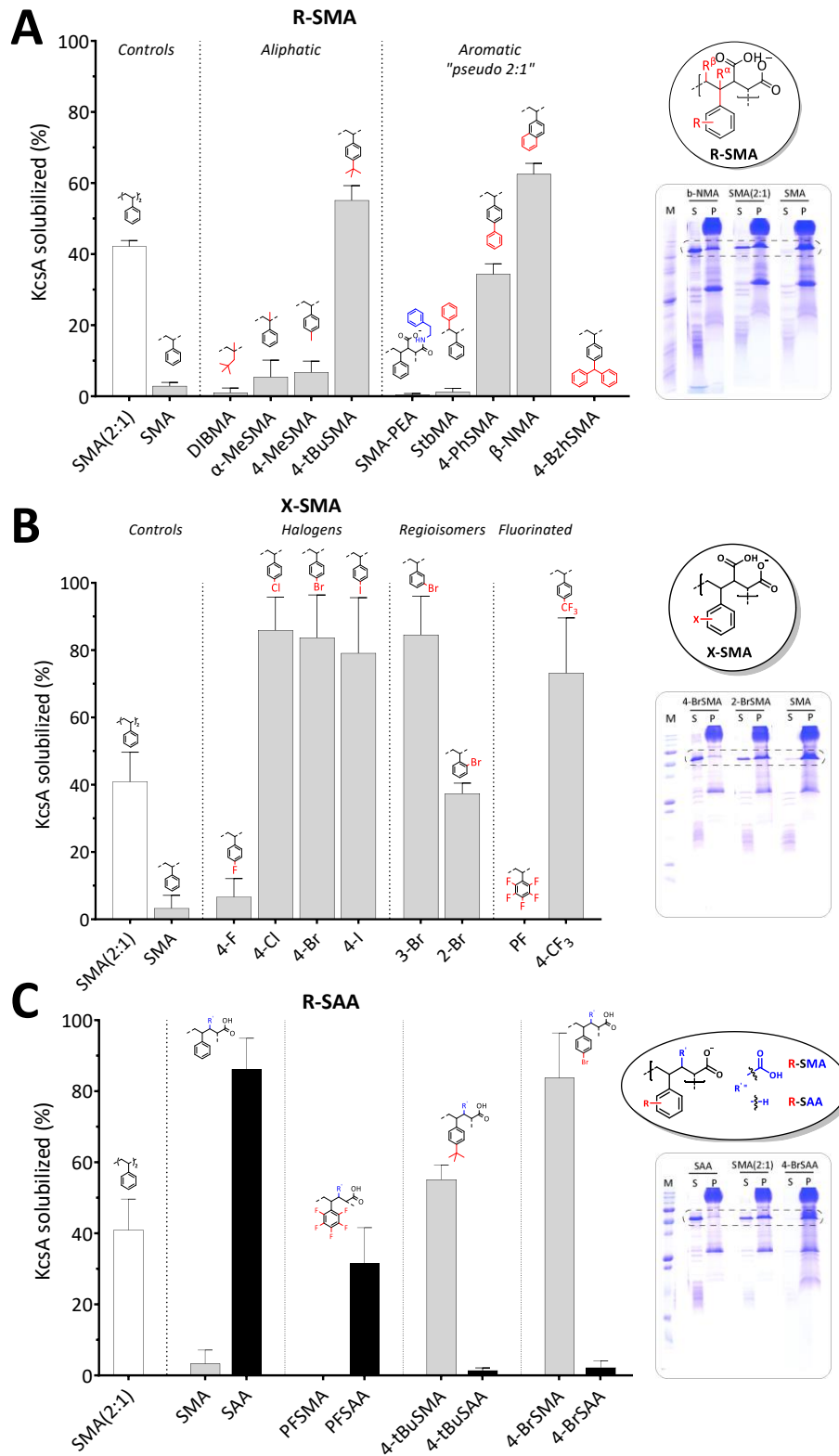


Fig. 2: Solubilization of the membrane protein, KcsA, from *E.coli* membranes by R-SMA (A), X-SMA (B), and R-SAA (C) copolymers. The general scaffolds are circled on the right, with deviations from styrene marked in red and depicted above the bars and deviations from the maleic acid moiety marked in blue. Inserts on the right show representative SDS-PAGE lanes for selected polymers (for complete overview see Fig. S5), with the dashed box highlighting the band corresponding to the KcsA tetramer. M, molecular weight marker; S, supernatant; P, pellet. KcsA solubilized (%) determined from the density of the KcsA band in S relative to the sum of S plus P. Data points indicate the mean  $\pm$ SD ( $n \geq 3$  independent experiments). Densitometry

data were obtained 2 hours post-solubilization at 25°C with a polymer concentration of 0.25% (w/v) (polymer-to-lipid ratio of ~2.3:1 (w/w)).

#### X-SMA halogenated analogues

A well-established phenomenon in the drug discovery field is that halogenation of compounds increases their lipophilicity<sup>[45]</sup> and enhances membrane binding and permeation.<sup>[46]</sup> This inspired us to synthesize a sub-set of R-SMA 1:1 copolymers bearing halogen substitutions (X-SMA). As shown in Fig. 2B, upon replacement of the proton at the 4-position with fluorine (the least hydrophobic halogen) the solubilization efficiency increases slightly but remains poor (7%). However, substitution with chlorine, bromine and iodine all result in a remarkable jump to near-complete solubilization (~86%, ~84% and ~79%, respectively).

The importance of the position of the substitutions was investigated by preparing regioisomers of BrSMA. While 3-BrSMA shows a similar high solubilization efficiency (~85%) as 4-BrSMA, for 2-BrSMA a ~two-fold drop in extraction efficiency (~37%) is observed, which still is comparable to that of 2:1 SMA (~41%).

To further probe substitution with fluorine, two more analogues were tested. Substitution of all aromatic protons by fluorine in perfluoro (PFSMA) resulted in a complete loss of MP extraction ability. Surprisingly, substitution by trifluoromethyl (4-CF<sub>3</sub>SMA) again resulted in a copolymer with very good solubilization capability (~73%).

#### R-SAA analogues

In the R-SAA set of polymers, the hydrophobicity of (1:1) SMA is increased by replacing the dicarboxylic acid in maleic acid (MA) by a monoacid derived from acrylic acid (AA), as first reported by Appel et al.<sup>[47]</sup> Fig. 2C shows that whereas SMA and PFSMA both are inefficient solubilizers, SAA is highly active and also PFSAA shows significant activity (~86% and ~32% extraction, respectively). By contrast, whereas 4-BrSMA and 4-tBuSMA are efficient solubilizers (~80% and ~55%, respectively), their acrylic acid equivalents, 4-BrSAA and 4-tBuSAA, both show negligible membrane protein extraction (<3%). Presumably, these acrylic variants are too hydrophobic, highlighting that a suitable hydrophobic balance is marked by sharp boundaries.

#### Efficiency of membrane solubilization in different systems as measured by turbidimetry

The membrane solubilizing efficacy of the copolymers thus far was based on extraction and quantification of KcsA from the *E.coli* inner membrane. We next explored turbidimetry as a more general approach to gain insight into the membrane solubilizing properties of the polymers.

#### Solubilization of biological membranes

Fig. 3A-C shows the percentage decrease in optical density (OD) after incubation with *E.coli* membranes for the three polymer sets. Importantly, for all three polymer sets good correlations are found when the percentage of KcsA extracted is plotted against the percentage decrease in OD (Fig. 3D-F), indicating that turbidimetry is a valuable tool to analyze solubilization efficiency. Notably, solubilization of *E.coli* membranes generally appears to be less efficient than KcsA extraction, likely because of the shorter incubation times and because the turbidimetry measurements also include outer *E.coli* membranes, which are more difficult to solubilize.

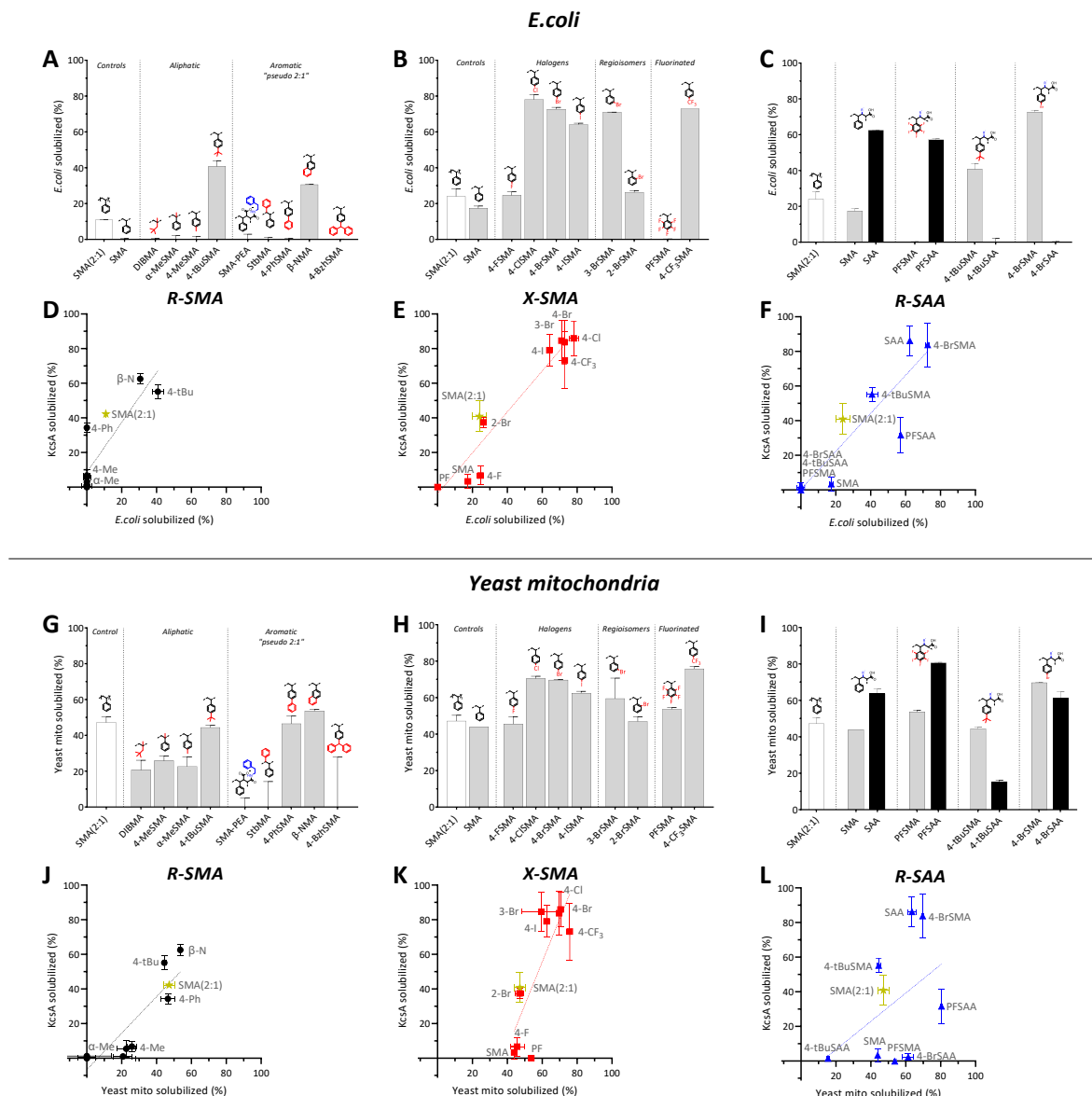


Fig. 3: Whole membrane solubilization as determined by turbidimetry for *E. coli* (A-C) and yeast mitochondria (G-I) and correlation with membrane protein (KcsA) extraction as determined by SDS-PAGE densitometry (D-F and J-L). The percentage of membrane solubilized is based on the relative decrease in optical density after 14 min (data are average of 2 independent experiments  $\pm$  range). Solubilization data are shown for analogues of R-SMA (left panels), X-SMA (middle panels) and R-SAA (right panels). Dashed lines indicate the line of linear fit. For the complete turbidimetry traces see Fig. S6.

Additional turbidimetry measurements on mitochondrial membranes from *Saccharomyces cerevisiae* showed that most of the polymers are able to also solubilize these yeast membranes (Fig. 3G-I). The polymers generally appear more efficient than with *E. coli* membranes, likely due to differences in membrane composition. For R-SMA and X-SMA, again good correlations are found with *E. coli* solubilization, while for R-SAA, rather surprisingly, the variation is much larger (Fig. 3J-L). The latter suggests that yeast membranes tolerate a broader hydrophobic balance range.

#### Solubilization of model lipid membranes

Model membranes are frequently used test systems to investigate the solubilization efficiency of amphipathic copolymers.<sup>[22][48][16]</sup> Here we used dimyristoylphosphatidylcholine (DMPC) vesicles at different temperatures (see Fig. S7 for traces and Fig. S8 for bar graphs) and plotted the solubilization

efficiency against that observed for *E.coli* inner membranes (based on KcsA extraction) and yeast mitochondrial membranes.

Fig. 4A shows that in the gel phase at 15°C there is a poor correlation between KcsA extraction and DMPC vesicle solubilization. For yeast membranes (Fig. 4C), which contain a substantial amount of PC lipids,<sup>[49][50]</sup> the correlation is much better, highlighting the importance of membrane properties for solubilization efficiency.<sup>[21][22]</sup> Strikingly, in the fluid phase at 30°C in both systems (Fig. 4 B and D), there is a sharp transition between poor solubilization and complete solubilization. Comparable results were observed for distearoylphosphatidylcholine (DSPC) vesicles, although solubilization in general was less efficient for these longer lipids (Fig. S9). These results suggest that polymers that are not able to efficiently solubilize DMPC or DSPC vesicles in the fluid phase can be considered poor biomembrane solubilizers. Hence, this may serve as a convenient screening assay to test new copolymers.

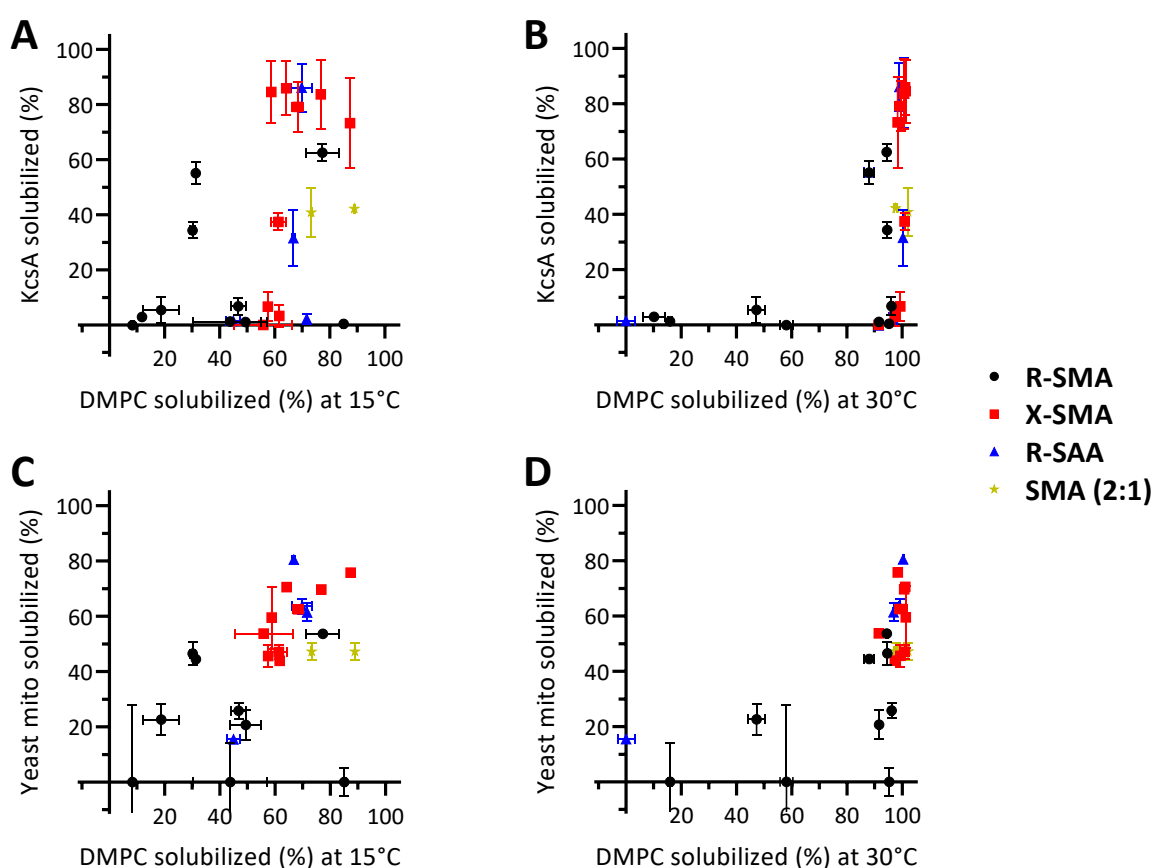


Fig. 4: Comparison of KcsA solubilization from *E.coli* (top) and yeast mitochondria solubilization (bottom) to model lipid-only vesicle solubilization. Data are shown for DMPC at 15°C (A, C) and 30°C (B, D). The different classes are depicted as follows: R-SMA, black circles; X-SMA, red squares; R-SAA, blue triangles. For systems  $T < T_M$  the vesicle solubilization rate was derived after 14 min, and for  $T > T_M$  time points were taken at 4 min (see Fig. S7 for turbidity traces and Fig. S8 for corresponding bar graphs).

### Nanoparticle sizes

From each set of copolymers we selected efficient solubilizers to compare the sizes of the purified KcsA nanodiscs by dynamic light scattering (DLS). As shown in Fig. 5A, most of the nanodiscs have a homogeneous size distribution and a small particle size of  $d \sim 8-10$  nm. Exceptions were the controls

of nanodiscs prepared from SMA (1:1), which were significantly larger ( $d \sim 30$  nm), and nanodiscs from SMA 2:1, which showed a less homogeneous size distribution.

When sizes of the KcsA nanodiscs are compared with those of nanoparticles solubilized from DMPC vesicles and copolymers only, the KcsA nanodiscs are larger (except for 4-CF<sub>3</sub>SMA) and the latter two appear to be rather similar (Fig. 5B). This was also observed for the other copolymers in the library (Fig. S10A). Likely, the excess copolymer contributes to the scattering, even though a relatively low polymer concentration was used. This is supported by the large apparent size difference for 4-CF<sub>3</sub>SMA between lipid-only nanodiscs and purified KcsA-containing nanodiscs (Fig. 5B). Furthermore, while it is not clear what determines the size of the polymer aggregates or the nanodiscs, we do note that polymers that form small aggregates in aqueous solution are the most efficient membrane solubilizers, with 4-CF<sub>3</sub>SMA and 3-BrSMA being the only exceptions (Fig. S10B).

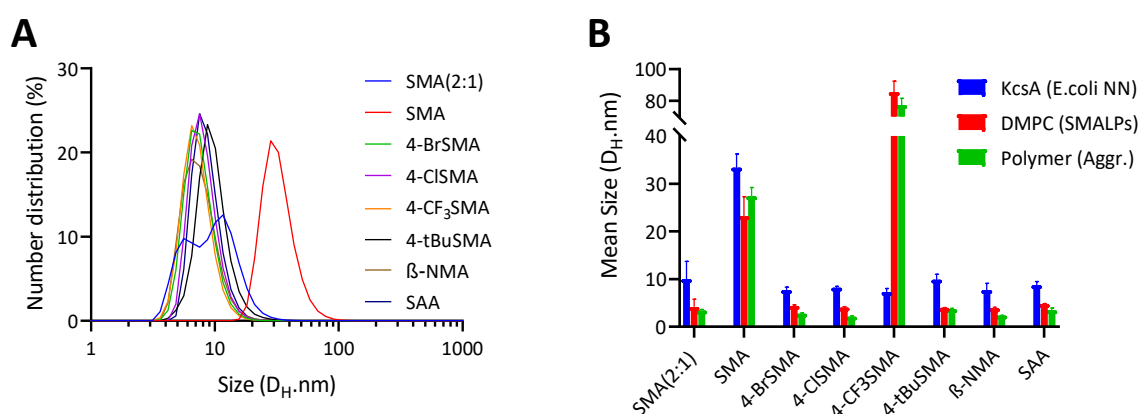


Fig. 5: DLS analysis of KcsA native nanodiscs (A) as well as DMPC nanodiscs and polymer aggregates (B). The values are the average from 7 measurements, with error bars reflecting the SD. Sizes are reported as the hydrodynamic diameters based on the peak maximum from the number-distributions. All samples contain ~0.4% (w/v) polymer, nanodisc samples also contain ~2 mM lipid (polymer-to-lipid ratio of ~3:1 (w/w)).

### Resistance against Ca<sup>2+</sup>-induced aggregation

For studies on membrane proteins, it can be useful when the copolymers tolerate the presence of divalent cations. Therefore, aggregation induced by titration with calcium ions was analysed by visual inspection and quantified by OD measurements (see Fig. S12). Table 2 shows that most of the copolymers precipitated in the low millimolar range ( $\leq 10$  mM). In agreement with literature,<sup>[43][51]</sup> DIBMA had a high resistance, remaining in solution up to ~40 mM Ca<sup>2+</sup>. Of the SMA analogues, only StbMA and  $\alpha$ -MeSMA showed high resistance to precipitation, up to calcium concentrations of ~45 mM and ~100 mM, respectively. Interestingly, these are the only three polymers with substitutions along the backbone: StbMA has a phenyl group on the  $\beta$  position, while DIBMA and  $\alpha$ -MeSMA have a methyl group on the  $\alpha$  position.

Table 2: Maximum tolerated concentration of calcium ions where no polymer precipitation was observed (see Fig. S12).

<i>R-SMA</i>	$[Ca^{2+}]$ (mM)	<i>X-SMA</i>	$[Ca^{2+}]$ (mM)	<i>R-SAA</i>	$[Ca^{2+}]$ (mM)
4-BzhSMA	<1	PFSMA	~2	4-BrSAA	~1
SMA-PEA	~2	4-ISMA	~3	4-tBuSAA	~1
$\beta$ -NMA	~5	3-BrSMA	~3	PFSAA	~3
4-PhSMA	~5	4-CF <sub>3</sub> SMA	~3	SAA	~5
4-MeSMA	~6	4-BrSMA	~4		
4-tBuSMA	~6	2-BrSMA	~5	<b>Controls</b>	$[Ca^{2+}]$ (mM)
DIBMA	~40	4-CISMA	~5	SMA(2:1)	~5
StbMA	~45	4-FSMA	~9	SMA(1:1)	~11
$\alpha$ -MeSMA	~100				

### Summary of relevant copolymer parameters

Here we will discuss how properties of the copolymer backbone and of the pendant chains may influence membrane solubilization and how this may help explain the results obtained from the three sets of copolymers.

#### Amphiphilicity

Acting at the interface between the hydrophobic fatty acid tails and the aqueous environment, the copolymers require a high degree of amphipathicity. They need to be sufficiently polar for solubility in water, and sufficiently hydrophobic to drive insertion into the membrane and to allow formation of stable nanodiscs. The balance between these two opposing parameters can be delicate, as clearly illustrated for example for the SAA analogues.

#### Flexibility of the backbone and pendant chains

In addition to amphipathicity, the copolymer must have sufficient flexibility to expose its hydrophilic groups to the aqueous phase and the hydrophobic groups to the lipid acyl chains without too many conformational constraints. This may be the reason why hydrophobic substituents on the pendant chains seem much more effective in increasing solubilization efficiency than hydrophobic substituents on the backbone, such as in the “pseudo 2:1 R-SMA polymers” SMA-PEA and StbMA, where the substitutions may interfere with backbone flexibility.

By contrast, for the pendant chains an increased rigidity may be advantageous for efficient solubilization, as it will reduce the loss of entropy upon membrane insertion. This can be achieved by having fewer rotatable bonds or more symmetrical substitutions, as in the  $\beta$ -NMA analogue or in the *para* substituted halogen analogues.

#### Size of the polymers and the pendant chains

Previously it was shown that copolymer sizes of <10 kDa are optimal for solubilization,<sup>[26][25]</sup> likely due to steric hindrance in longer polymers and a tendency to form aggregates in the aqueous phase. This is in line with our present observation that copolymers that form larger aggregates in solution generally are less efficient solubilizers.

Also for the pendant groups size plays an important role. To allow insertion into the membrane, a smaller size might be beneficial, combined with sufficient hydrophobicity. However, the formation of nanodiscs should be more favourable than insertion at the interface and therefore the polymer should also be able to disrupt lipid packing. This may be promoted by a larger size of the pendant chain or deeper penetration into the bilayer. Possibly, the halogen analogues as studied here strike an optimal

balance, as they can introduce significant lipophilicity with an intermediate bulk and size and can efficiently solubilize a range of target membranes with different lipid packing properties.

#### Positioning of substitutions on backbone and pendant chains

Additional (hydrophobic) substituents on the backbone (i.e. DIBMA,  $\alpha$ -MeSMA and StbMA) do not result in efficient solubilization under the suboptimal environmental conditions used here. However, as demonstrated for DIBMA,<sup>[43][51]</sup> at higher concentrations such analogues may be very useful for biological systems, in particular since they tolerate divalent cations. The reason for this tolerance is likely that steric hindrance prevents chelation of the cations to the carboxyl groups, either directly by physically obstructing access, or by changing the backbone conformation and flexibility.

Also for the pendant groups the positioning of substituents is important. Attachment of the derivative on the 3- and 4-position of the phenyl ring is superior to the 2-position, as shown for the brominated SMA analogues. Possible reasons are that the closeness of the 2-position to the backbone results in steric hindrance, reducing the conformational freedom of the polymer backbone and/or that a deeper penetration into the hydrophobic core for the 3- and 4-positions facilitates membrane disruption.

#### Electronic effects

Phenyl groups have an electronic surface potential that is negative above and below the ring and positive in the plane of the ring.<sup>[52]</sup> This may play a role in membrane insertion of styrene-containing polymers, in particular since the membrane core has a positive dipole potential.<sup>[53][54]</sup> Halogens generally have high electronegativities and are electron-withdrawing, thereby modifying the electrostatic surface potential of the aromatic rings.<sup>[55]</sup> It is not clear how this would affect insertion, but we do note that substitution with F, which is the most electronegative element in the periodic table, does not result in efficient solubilization. Another property of the heavier halogens (Cl, Br, I) is that they have an electrostatically positive region ( $\sigma$ -hole) that can act as a Lewis acid and undergo halogen bonding with nucleophiles,<sup>[56][57]</sup> either within the copolymer molecule(s) themselves or with lipids and proteins.

#### Implications for polymer design

The solubilization efficiency of any copolymer obviously will depend on the membrane environment and on environmental parameters. However, for maximum solubilization efficiency in a wide range of target membranes under the conditions used here, the halogen substitutions seem most promising, together with the naphthalene variant and SAA polymers. Substitutions on the backbone on the other hand may improve activity in the presence of divalent cations. Although beyond the scope of this work, it should be noted that varying copolymer properties may affect the functionality of membrane proteins.<sup>[58]</sup>

The new library of copolymers offers several advantages over commercially available copolymers. First, the copolymers in the present study are well-defined in terms of sequence distribution and size, which is useful for systematic studies to understand their mode of action. For example, it will help molecular dynamics simulations as it allows a more accurate representation of the polymers. Furthermore, through the size control of RAFT polymerization, copolymers can be employed without interference (band smearing) of longer copolymers on SDS gels. RAFT synthesized copolymers in addition have the potential to be selectively modified on the end groups, allowing incorporation of a single label such as a fluorophore or affinity-tag per copolymer molecule. Last but not least, halogenated copolymers may be useful for dedicated biophysical techniques, e.g. the use of (i) fluorinated copolymers, such as 4-CF<sub>3</sub>SMA, for <sup>19</sup>F-NMR studies, (ii) brominated copolymers for MS experiments due to their convenient isotopic signature, and (iii) copolymers with heavier halogens

(i.e. 4-BrSMA or 4-ISMA) for EM microscopy where the polymers/particles could potentially be visualized more easily due to the scattering of the dense halogen atoms.

## Conclusion

We have introduced a library of poly(styrene-*alt*-maleic/acrylic acid) analogues, with well-defined composition and length. The library contains several promising new analogues with equivalent or better membrane protein solubilization when compared to the benchmark of 2:1 SMA (Xiran30010). By systematic variation of nature and positioning of different substituents, we obtained new insights into the parameters that govern efficient solubilization and tolerance of divalent cations. This knowledge can be utilized for the targeted and rational design of future copolymer generations for membrane protein solubilization. In addition, the library expands the toolbox for the study of membrane proteins, allowing improvement of yields and stability of precious membrane protein samples.

## Acknowledgements

We are grateful to Helene Jahn for providing the yeast mitochondrial membranes, Bonny W. M. Kuipers for support in DLS analysis, as well as Polyscope Polymers (NL) for gifting the (2:1) SMA<sub>h</sub> copolymer (Xiran SZ30010). This work was supported financially by the Division of Chemical Sciences (CW) of the Netherlands Organisation for Scientific Research (NWO) via ECHO grant No. 711-017-006 (A.H.K).

## References

- [1] F. Li, P. F. Egea, A. J. Vecchio, I. Asial, M. Gupta, J. Paulino, R. Bajaj, M. S. Dickinson, S. Ferguson-Miller, B. C. Monk, R. M. Stroud, *J. Biol. Chem.* **2021**, *296*, 100557.
- [2] M. N. Mbaye, Q. Hou, S. Basu, F. Teheux, F. Pucci, M. Rooman, *Sci. Rep.* **2019**, *9*, 1–14.
- [3] T. J. Knowles, M. Overduin, R. Finka, C. Smith, Y.-P. Lin, T. Dafforn, *J. Am. Chem. Soc.* **2009**, *22*, 7484–7485.
- [4] I. Prabudiansyah, I. Kusters, A. Caforio, A. J. M. Driessen, *Biochim. Biophys. Acta - Biomembr.* **2015**, *1848*, 2050–2056.
- [5] C. Sun, S. Benlekbir, P. Venkatakrishnan, Y. Wang, S. Hong, J. Hosler, E. Tajkhorshid, J. L. Rubinstein, R. B. Gennis, *Nat. Lett.* **2018**, *557*, 123–126.
- [6] S. C. Lee, T. J. Knowles, V. L. G. Postis, M. Jamshad, R. A. Parslow, Y. P. Lin, A. Goldman, P. Sridhar, M. Overduin, S. P. Muench, T. R. Dafforn, *Nat. Protoc.* **2016**, *11*, 1149–1162.
- [7] J. M. Dörr, M. C. Koorengevel, M. Schäfer, A. V Prokofyev, S. Scheidelaar, E. A. W. van der Cruijssen, T. R. Dafforn, M. Baldus, J. A. Killian, *PNAS* **2014**, *111*, 18607–18612.
- [8] D. J. K. Swainsbury, S. Scheidelaar, R. Van Grondelle, J. A. Killian, M. R. Jones, *Angew. Chemie - Int. Ed.* **2014**, *53*, 11803–11807.
- [9] E. Calzada, E. Avery, P. N. Sam, A. Modak, C. Wang, J. M. Mccaffery, X. Han, N. N. Alder, S. M. Claypool, *Nat. Commun.* **2019**, *10*.
- [10] A. C. K. Teo, S. C. Lee, N. L. Pollock, Z. Stroud, S. Hall, A. Thakker, A. R. Pitt, T. R. Dafforn, C. M. Spickett, D. I. Roper, *Sci. Rep.* **2019**, *9*, 1–10.
- [11] N. Hellwig, O. Peetz, Z. Ahdash, I. Tascón, P. J. Booth, V. Mikusevic, M. Diskowski, A. Politis, Y. Hellmich, I. Hänel, E. Reading, N. Morgner, *Chem. Commun.* **2018**, *54*, 13702–13705.

- [12] M. Overduin, C. Trieber, R. S. Prosser, L. P. Picard, J. G. Sheff, *Membranes (Basel)*. **2021**, *11*, 1–20.
- [13] E. Reading, Z. Hall, C. Martens, T. Haghghi, H. Findlay, Z. Ahdash, A. Politis, P. J. Booth, *Angew. Chemie - Int. Ed.* **2017**, *56*, 15654–15657.
- [14] A. Olerinyova, A. Sonn-Segev, J. Gault, C. Eichmann, J. Schimpf, A. H. Kopf, L. S. P. Rudden, D. Ashkinadze, R. Bomba, L. Frey, J. Greenwald, M. T. Degiacomi, R. Steinhilper, J. A. Killian, T. Friedrich, R. Riek, W. B. Struwe, P. Kukura, *Chem* **2021**, *7*, 224–236.
- [15] B. Bersch, J. M. Dörr, A. Hessel, J. A. Killian, P. Schanda, *Angew. Chemie - Int. Ed.* **2017**, *56*, 2508–2512.
- [16] T. Ravula, S. K. Ramadugu, G. Di Mauro, A. Ramamoorthy, *Angew. Chemie - Int. Ed.* **2017**, *56*, 11466–11470.
- [17] M. Parmar, S. Rawson, C. A. Scarff, A. Goldman, T. R. Dafforn, S. P. Muench, V. L. G. Postis, *Biochim. Biophys. Acta - Biomembr.* **2018**, *1860*, 378–383.
- [18] I. Tascón, J. S. Sousa, R. A. Corey, D. J. Mills, D. Griwatz, N. Aumüller, V. Mikusevic, P. J. Stansfeld, J. Vonck, I. Hänelt, *Nat. Commun.* **2020**, *11*, 1–10.
- [19] A. H. Kopf, J. M. Dörr, M. C. Koorengel, F. Antoniciello, H. Jahn, J. A. Killian, *Biochim. Biophys. Acta - Biomembr.* **2020**, *1862*, 183125.
- [20] S. Scheidelaar, M. C. Koorengel, C. A. Van Walree, J. J. Dominguez, J. M. Dörr, J. A. Killian, *Biophys. J.* **2016**, *111*, 1974–1986.
- [21] J. J. Dominguez Pardo, J. M. Dörr, A. Iyer, R. C. Cox, S. Scheidelaar, M. C. Koorengel, V. Subramaniam, J. A. Killian, *Eur. Biophys. J.* **2017**, *46*, 91–101.
- [22] S. Scheidelaar, M. C. Koorengel, J. J. Dominguez Pardo, J. D. Meeldijk, E. Breukink, J. A. Killian, *Biophys. J.* **2015**, *108*, 279–290.
- [23] K. Janson, J. Zierath, F. L. Kyrilis, A. Dmitry, F. Hamdi, I. Skalidis, A. H. Kopf, M. Das, C. Kolar, M. Rasche, C. Vargas, S. Keller, P. L. Kastiris, A. Meister, *BBA - Biomembr.* **2021**, 183725.
- [24] R. D. Cunningham, A. H. Kopf, B. O. W. Elenbaas, B. B. P. Staal, R. Pfukwa, J. A. Killian, B. Klumperman, *Biomacromolecules* **2020**, *21*, 3287–3300.
- [25] D. J. K. Swainsbury, S. Scheidelaar, N. Foster, R. Van Grondelle, J. A. Killian, M. R. Jones, *BBA - Biomembr.* **2017**, *1859*, 2133–2143.
- [26] K. A. Morrison, A. Akram, A. Mathews, Z. A. Khan, J. H. Patel, C. Zhou, D. J. Hardy, C. Moore-Kelly, R. Patel, V. Odiba, T. J. Knowles, M. -u.-H. Javed, N. P. Chmel, T. R. Dafforn, A. J. Rothnie, *Biochem. J.* **2016**, *473*, 4349–4360.
- [27] J. J. Domínguez Pardo, M. C. Koorengel, N. Uwugiaren, J. Weijers, A. H. Kopf, H. Jahn, C. A. van Walree, M. J. van Steenberg, J. A. Killian, *Biophys. J.* **2018**, *115*, 129–138.
- [28] A. Grethen, A. O. Oluwole, B. Danielczak, C. Vargas, S. Keller, *Sci. Rep.* **2017**, *7*, 1–14.
- [29] J. M. Dörr, S. Scheidelaar, M. C. Koorengel, J. J. Dominguez, M. Schäfer, C. A. van Walree, J. A. Killian, *Eur. Biophys. J.* **2016**, *45*, 3–21.
- [30] D. J. T. Hill, J. H. O. Donnell, P. W. O. Sullivan, O. Donnell, O. Sullivan, *Macromolecules* **1985**, *18*, 9–17.
- [31] B. Klumperman, *Polym. Chem.* **2010**, *1*, 558–562.

- [32] M. Zhu, L. Wei, M. Li, L. Jiang, F. Du, Z. Li, F. Li, *Chem Comm* **2001**, 365–366.
- [33] B. D. Harding, G. Dixit, K. M. Burrige, I. D. Sahu, C. Dabney-, R. E. Edelman, D. Konkolewicz, G. A. Lorigan, *Chem Phys Lipids* **2019**, 65–72.
- [34] S. C. L. Hall, C. Tognoloni, G. J. Price, B. Klumperman, K. J. Edler, T. R. Da, T. Arnold, *Biomacromolecules* **2018**, 761–772.
- [35] A. A. A. Smith, H. E. Autzen, T. Laursen, V. Wu, M. Yen, A. Hall, S. D. Hansen, Y. Cheng, T. Xu, *Biomacromolecules* **2017**, *18*, 3706–3713.
- [36] M. Esmaili, C. Acevedo-Morantes, H. Wille, M. Overduin, *Biochim. Biophys. Acta - Biomembr.* **2020**, *1862*, 183360.
- [37] N. G. Brady, C. E. Workman, B. Cawthon, B. D. Bruce, B. K. Long, *Biomacromolecules* **2021**, *22*, 2544–2553.
- [38] N. Z. Hardin, T. Ravula, G. Di Mauro, A. Ramamoorthy, *Small* **2019**, *15*, 1–5.
- [39] T. Ravula, N. Z. Hardin, S. K. Ramadugu, S. J. Cox, A. Ramamoorthy, *Angew. Chemie - Int. Ed.* **2018**, *57*, 1342–1345.
- [40] M. C. Fiori, Y. Jiang, G. A. Altenberg, H. Liang, *Sci. Rep.* **2017**, *7*, 1–10.
- [41] N. Z. Hardin, V. Kocman, G. M. Di Mauro, T. Ravula, A. Ramamoorthy, *Angew. Chemie - Int. Ed.* **2019**, *58*, 17246–17250.
- [42] T. Ravula, N. Z. Hardin, S. K. Ramadugu, A. Ramamoorthy, *Langmuir* **2017**, *33*, 10655–10662.
- [43] A. O. Oluwole, B. Danielczak, A. Meister, J. O. Babalola, C. Vargas, S. Keller, *Angew. Chemie - Int. Ed.* **2017**, *56*, 1919–1924.
- [44] M. Esmaili, C. J. Brown, R. Shaykhutdinov, C. Acevedo-Morantes, Y. L. Wang, H. Wille, R. D. Gandour, S. R. Turner, M. Overduin, *Nanoscale* **2020**, *12*, 16705–16709.
- [45] A. Priimagi, G. Cavallo, P. Metrangolo, G. Resnati, *Acc. Chem. Res.* **2013**, *46*.
- [46] G. Gerebtzoff, X. Li-blatter, H. Fischer, A. Frentzel, A. Seelig, *ChemBioChem* **2004**, 676–684.
- [47] A. A. A. Smith, H. E. Autzen, B. Faust, J. L. Mann, B. W. Muir, S. Howard, A. Postma, A. J. Spakowitz, Y. Cheng, E. A. Appel, *Chem* **2020**, *6*, 2782–2795.
- [48] R. C. Arenas, J. Klingler, C. Vargas, S. Keller, *Nanoscale* **2016**, *8*, 15016–15026.
- [49] H. A. Boumann, M. J. A. Damen, C. Versluis, A. J. R. Heck, B. De Kruijff, A. I. P. M. De Kroon, *Biochemistry* **2003**, *42*, 3054–3059.
- [50] S. E. Horvath, G. Daum, *Prog. Lipid Res.* **2013**, *52*, 590–614.
- [51] B. Danielczak, A. Meister, S. Keller, *Chem. Phys. Lipids* **2019**, *221*, 30–38.
- [52] A. Dhotel, Z. Chen, L. Delbreilh, B. Youssef, J. Saiter, L. Tan, *Int. J. Mol. Sci.* **2013**, *14*, 2303–2333.
- [53] H. Brockman, *Chem. Phys. Lipids* **1994**, *73*, 57–79.
- [54] J. Cladera, P. O’Shea, *Biophys. J.* **1998**, *74*, 2434–2442.
- [55] Y. Lu, Y. Liu, Z. Xu, H. Li, H. Liu, W. Zhu, *Expert Opin. Drug Discov.* **2012**, *7*, 375–383.
- [56] P. Auffinger, F. A. Hays, E. Westhof, P. S. Ho, *Proc. Natl. Acad. Sci.* **2004**, *101*, 16789–16794.

- [57] R. Wilcken, M. O. Zimmermann, A. Lange, A. C. Joerger, F. M. Boeckler, *J. Med. Chem.* **2013**, *56*, 1363–1388.
- [58] R. L. Grime, R. T. Logan, S. A. Nestorow, P. Sridhar, P. C. Edwards, C. G. Tate, B. Klumperman, T. R. Dafforn, D. R. Poyner, P. J. Reeves, M. Wheatley, *Nanoscale* **2021**.